

# Inclusion of Aminobenzonitrile Isomers by a Diol Host Compound: Structure and Selectivity

Mino R. Caira,<sup>†</sup> Luigi R. Nassimbeni,<sup>\*,†</sup> Fumio Toda,<sup>‡</sup> and Dejana Vujovic<sup>†</sup>

Contribution from the Departments of Chemistry, University of Cape Town, Rondebosch 7701, South Africa, and Faculty of Science, Okayama University of Science, 1-1 Ridaicho, Okayama 700-0005, Japan

Received November 19, 1999. Revised Manuscript Received July 10, 2000

**Abstract:** 1,1,6,6-Tetraphenylhexa-2,4-diyne-1,6-diol (**H**) forms inclusion compounds with 2-, 3-, and 4-aminobenzonitrile (2ABN, 3ABN, and 4ABN). In each case the host:guest ratio is 1:2 and the structures are stabilized by hydrogen bonds. Competition experiments show that the host selects the guests in order of preference of 2ABN > 3ABN > 4ABN. These results are in general agreement with lattice energy calculations, thermal analyses, and solid-state reactions. The structure of the solid formed between **H** and a mixture of 3ABN and 4ABN has also been elucidated.

## Introduction

The process of molecular recognition lies at the heart of host–guest chemistry, because it is the nonbonded intermolecular interactions which are responsible for such phenomena as self-assembly of molecules,<sup>1</sup> cooperative phenomena in biological macromolecules,<sup>2</sup> and the equilibria established between proteins and ligands.<sup>3</sup> Herbstein<sup>4</sup> has given a classification scheme for binary adducts A–B which distinguishes between “enclosure, segregated stack and packing complexes”, and “molecular compounds”, depending on the relative strengths of A···A or A···B intermolecular interactions. Weber’s classification of host–guest compounds took into account the types of interaction, stoichiometry, and topology of the inclusion compounds.<sup>5</sup> Hydrogen bonding remains the most important molecular interaction and two recent books review the subject and have extensive bibliographies.<sup>6,7</sup> Selective enclathration is an excellent example of molecular recognition, because the subtle differences in the strength and direction of host–guest interactions can be sufficient for a given host molecule to encapsulate one particular isomer from a mixture of guests. We have used a variety of bulky diol host molecules to separate isomers of the phenylene–diamines, benzenediols, picolines, and lutidines.<sup>8</sup> We now present the results of the structural analyses and competition experiments obtained from the inclusion of the isomers of

aminobenzonitriles by 1,1,6,6-tetraphenylhexa-2,4-diyne-1,6-diol (see Scheme 1).

## Results and Discussion

**Competition Experiments.** The results of the competition experiments are illustrated in Figure 1. Each two-component experiment shows the mole fraction *X* of a given guest in the initial solution versus the mole fraction *Z* of the guest included by the host.

We note that in each case the selectivity is concentration dependent. In particular in the 2ABN versus 3ABN the former is favored when  $X(2ABN) > 0.2$  (Figure 1a). Similar results obtain in the competition of 2ABN versus 4ABN (Figure 1b). However, in the case of 3ABN versus 4ABN, the results are totally concentration dependent, with negligible selectivity occurring at  $X(3ABN) = 0.5$  (Figure 1c).

The three-component experiment is shown on the equilateral triangle, the three apexes of which represent the pure component aminobenzonitriles (Figure 1d). We selected starting mixtures represented by the circles and the resulting mixtures move in the direction indicated by the arrows, to the final compositions near the apexes labeled 2ABN and 3ABN. We see that for almost all starting mixtures there is a pronounced migration toward 2ABN, but that if the initial mixture has  $X(3ABN) > 0.67$ , then the latter is enriched.

**Structures.** Crystal and experimental data are given in Table 1.

For **1**, the space group is  $P2_1/c$  with  $Z = 2$ , so the host is located on a center of inversion at Wyckoff position *c*, while the guest molecules are in general positions. The host molecules are packed in rows in the [100] direction and the guests are located in channels running parallel to [100]. This is illustrated in Figure 2a,b, which shows a projection of the structure as well as a space-filling projection with the guest molecules removed demonstrating the geometry of the channels. The hydroxyl moieties act as both hydrogen bonding donors and acceptors. Thus we have (Guest)N–H···OH(Host) with  $d(N···O) = 3.193 \text{ \AA}$  and (Host)O–H···N≡C(Guest) with  $d(O···N) = 2.891 \text{ \AA}$ . This is illustrated in Figure 3. Thus the 2ABN guests act as a bridge between adjacent host molecules,

<sup>†</sup> University of Cape Town.

<sup>‡</sup> Okayama University of Science.

(1) Orr, W. G.; Barbour, L. J.; Atwood, J. L. *Science* **1999**, *285*, 1049–1052.

(2) Di Cera, E. *Chem. Rev.* **1998**, *98*, 1563–1591.

(3) Rabine, R. E.; Bender, S. L. *Chem. Rev.* **1997**, *97*, 1359–1472.

(4) Herbstein, F. H. *Acta Chim. Hung.* **1993**, *130*, 377–386.

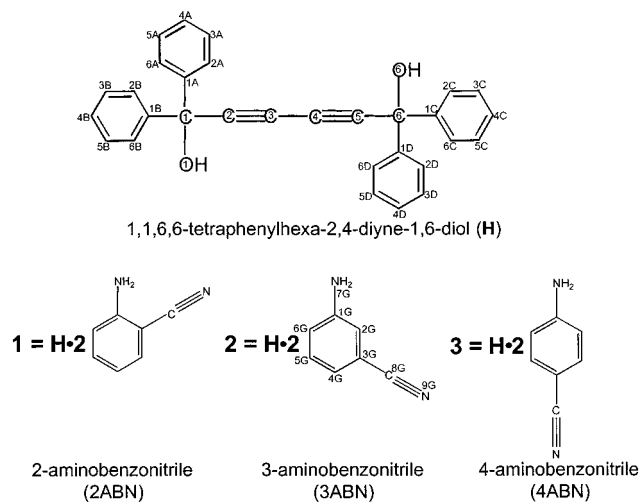
(5) Weber, E.; Josel, H.-P. *J. Inclusion Phenom.* **1983**, *1*, 79–85.

(6) Jeffrey, G. A. *An Introduction to Hydrogen Bonding*; Oxford University Press: Oxford, 1997.

(7) Desiraju, G. R.; Steiner, T. *The Weak Hydrogen Bond in Structural Chemistry and Biology*; IUCr Monographs on Crystallography 9; Oxford University Press: Oxford, 1999.

(8) (a) Caira, M. R.; Horne, A.; Nassimbeni, L. R.; Toda, F. *J. Chem. Soc., Perkin 2* **1995**, 1063–1067. (b) Caira, M. R.; Horne, A.; Nassimbeni, L. R.; Toda, F. *J. Chem. Soc., Perkin 2* **1997**, 1717–1720. (c) Caira, M. R.; Horne, A.; Nassimbeni, L. R.; Toda, F. *J. Mater. Chem.* **1997**, *7*, 2145–2149. (d) Caira, M. R.; Horne, A.; Nassimbeni, L. R.; Toda, F. *Supramol. Chem.* **1998**, *9*, 231–237.

## Scheme 1



giving rise to infinite  $(\text{H} \cdots \text{G} \cdots \text{H} \cdots \text{G})_n$  hydrogen-bonded chains running parallel to [100].

For **2** and **3**, the space group is  $P\bar{1}$ , with  $Z = 1$ . In both cases the host molecules are located on the centers of inversion (Wyckoff position  $h$  for **2** and Wyckoff position  $a$  for **3**), while the guest molecules are in general positions. As in the case for **1**, host molecules of **2** and **3** pack in the [100] direction, while guest molecules are located in channels parallel to the  $a$ -axis. Each channel contains two rows of guest molecules (Figures 4 and 5). Hydrogen bonding of **2** and **3** is quite different from that of **1**. Here the nitrile group acts as a double H-bond acceptor, forming two hydrogen bonds, one with the hydroxyl group of the host and one with the amine group of another guest.

The arrangement of guest molecules in **2** is different from that in **3**, giving rise to hydrogen-bonded (Guest) $\cdots$ (Guest) chains with distinct geometries. These are shown in Figures 6 and 7 and details of the hydrogen-bonding parameters are given in Table 2.

We have also analyzed the topology of the channels, in which guest molecules are located, using the program SECTION.<sup>9</sup> The cross-sectional area of the channels varies from  $3.5 \times 8.1$  to  $4.3 \times 10.0$  Å for **1**, from  $4.3 \times 5.9$  to  $6.3 \times 11.1$  Å for **2**, and from  $4.1 \times 7.9$  to  $9.7 \times 9.4$  Å for **3**. These dimensions give some impression of the variations in cross-sectional areas of the channels.

**Lattice Energy Calculations.** Lattice energy calculations were performed for **1**, **2**, and **3** using the atom–atom potential method. We employed the program HEENY,<sup>10</sup> using a force field of the type

$$V(r) = a \exp(-br) - c/r^6$$

where  $r$  is the interatomic distance and the coefficients  $a$ ,  $b$ , and  $c$  are those given by Gavezzotti.<sup>11</sup> We incorporated a hydrogen-bonding potential, which is a simplified version of that given by Vedani and Dunitz<sup>12</sup> and is formulated as

$$V(\text{H-bond}) = (A/R^{12} - C/R^{10}) \cos^2 \theta$$

where  $R$  is the distance between the hydroxyl or amino hydrogen and the N acceptor.  $\theta$  is the Donor–H $\cdots$ N angle, and the  $\cos^2 \theta$

term is the energy penalty paid by the bond to take nonlinearity into account. We selected a representative host–guest pair and carried out appropriate summations of all host $\cdots$ host, host $\cdots$ guest, and guest $\cdots$ guest interactions. We obtained the following values for the lattice energies: **1**,  $-550.7$  kJ/mol; **2**,  $-504.1$  kJ/mol; and **3**,  $-489.0$  kJ/mol. This outcome is gratifying, in that it shows that the stabilities of the inclusion complexes are in the order **1** > **2** > **3**. This is in agreement with the major results obtained in the 3-component competition experiments, in that in the three-component system 4-aminobenzonitrile is always disfavored and the majority of starting mixtures migrate toward 2-aminobenzonitrile.

We note, however, that the lattice energies of **2** (3-aminobenzonitrile) and **3** (4-aminobenzonitrile) are close; they only differ by 15.1 kJ/mol (3.1 kcal/mol) and we believe that this and the kinetic effects are responsible for the strong concentration dependence of 3ABN versus 4ABN competition experiments.

**Thermal Analysis.** While TG is generally an excellent method of obtaining the host:guest ratio in inclusion compounds, particularly when the guests are volatile, in this case we obtained no definitive mass loss because all three compounds decomposed beyond 140 °C. The DSC experiments each yielded a single endotherm which we attribute to the dissolution of the host compound in the guest. Details of the onset temperatures, peak temperatures, enthalpies of dissolution, and computed lattice energies are given in Table 3. We note that the most stable compound, **1**, has the most negative lattice energy and the highest temperature and enthalpy of dissolution. Results for the other two compounds (Table 3) follow a trend.

**Mixed Crystal.** We grew a large single crystal of the host with a mixture of 3ABN and 4ABN (**MIX**). The size of the crystal ( $2 \times 2 \times 0.5$  mm<sup>3</sup>) allowed us to cut it into two portions, one of which was used for X-ray analysis and the other for GC. The latter established the 3ABN:4ABN ratio to be 57%:43%.

The crystal data (Table 1) show that the unit cell parameters of **MIX** and **3** are very similar. The positions of the host atoms were found by direct methods, and when these were allowed to refine, the positions of the mixed guest appeared in a difference electron density map. The position of the nitrile nitrogen N8G was clearly identified and it is hydrogen bonded to the hydroxyl hydrogen of the host. The amino nitrogens were both clearly present and we refined them with site occupancies of 0.57 and 0.43 as determined by GC analysis. The amino hydrogens, however, could not be located and were not incorporated into the final model. The hydrogen-bonded motif of **MIX** is shown in Figure 8.

**Solid–Solid Reactions.** Reactions of organic compounds in the solid state have largely focused on molecular crystals, and photochemical reactions in solids have often yielded different products from those obtained in solution, owing to the physical restraints imposed by the crystal packing. Pioneering work in this field was carried out by Schmidt and co-workers, who formulated the geometric rules for photocycloaddition.<sup>13</sup> More recently, Scheffer has demonstrated the versatility of solid-state organic photochemistry, by applying this technique to a variety of synthetic procedures.<sup>14</sup> Structural control of organic crystals and their concomitant reactivity is a topic of current interest in crystal engineering. In particular Aoyama has discussed catalysis

(13) Schmidt, G. M. J. *Pure Appl. Chem.* **1971**, 27, 674.

(9) SECTION, a computer program for the graphic display of cross sections through a unit cell: Barbour, L. J. *J. Appl. Cryst.* **1999**, 32, 353.

(10) Motherwell, W. D. S. *EENY*, Potential Energy Program, Cambridge University.

(11) Gavezzotti, A. *Crystallogr. Rev.* **1998**, 7, 5.

(12) Vedani, A.; Dunitz, J. D. *J. Am. Chem. Soc.* **1985**, 107, 7653.

(14) (a) Gundmundsdottir, A. D.; Scheffer, J. R.; Trotter, J. *Tetrahedron Lett.* **1994**, 35, 1397. (b) Gamlin, J. N.; Jones, R.; Leibovitch, M.; Patrick, B.; Scheffer, J. R.; Trotter, *J. Acc. Chem. Res.* **1996**, 29, 203. (c) Leibovitch, M.; Olovsson, G.; Scheffer, J. R.; Trotter, *J. Pure Appl. Chem.* **1997**, 69, 815.

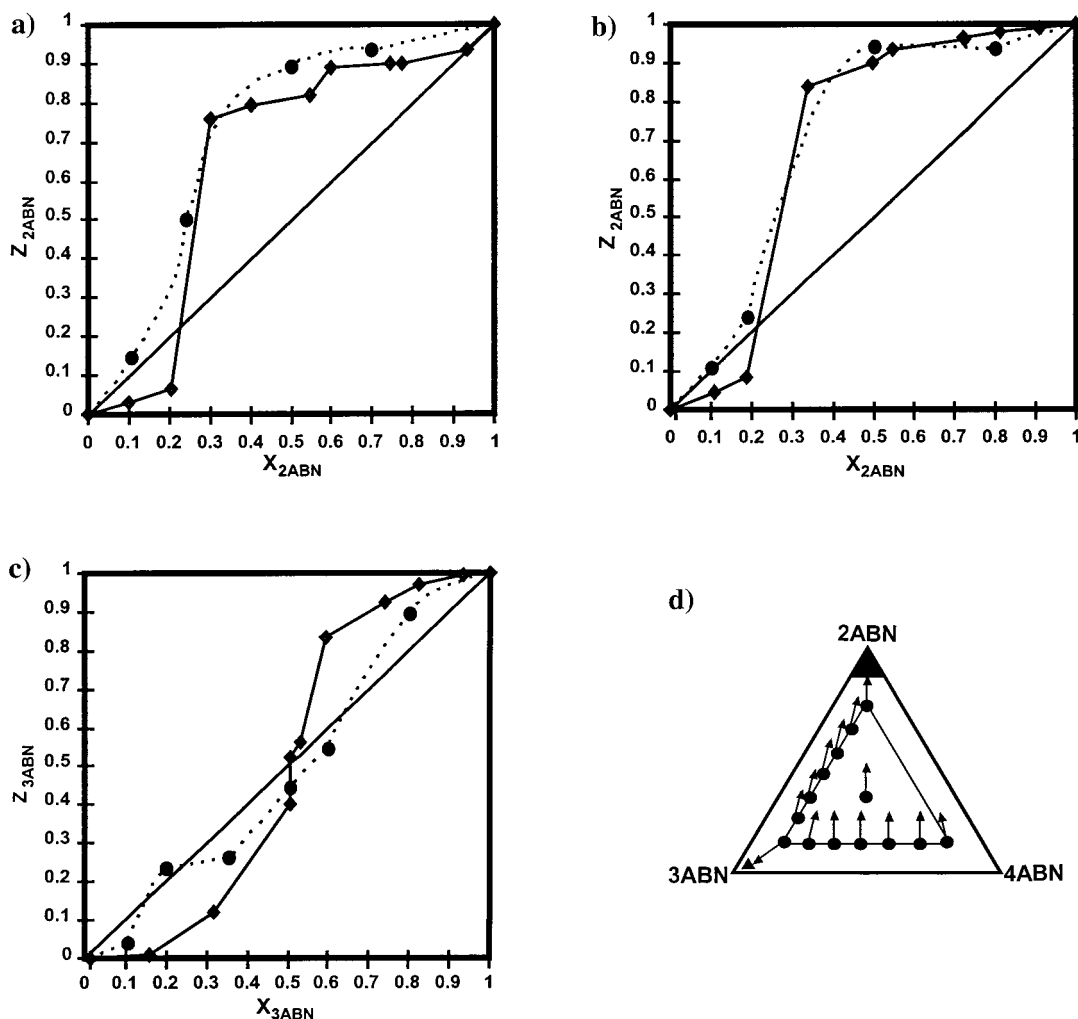


**Figure 1.** Results of the competition experiments: (a) 2ABN versus 3ABN, (b) 2ABN versus 4ABN, (c) 3ABN versus 4ABN, and (d) three component competition in solution. Solid lines show results of solution experiments and broken lines those from solid–solid reactions.

**Table 1.** Crystal Data and Experimental and Refinement Parameters

inclusion compd	1	2	3	MIX
molecular formula	$C_{30}H_{22}O_2 \cdot 2C_7H_6N_2$	$C_{30}H_{22}O_2 \cdot 2C_7H_6N_2$	$C_{30}H_{22}O_2 \cdot 2C_7H_6N_2$	$C_{30}H_{22}O_2 \cdot (3ABN) \cdot (4ABN)$
$M_r/g \cdot mol^{-1}$	650.75	650.75	650.75	650.75
$T/K$	185(2)	293(2)	173(2)	148(2)
crystal system	monoclinic	triclinic	triclinic	triclinic
space group	$P2_1/c$	$P\bar{1}$	$P\bar{1}$	$P\bar{1}$
$a/\text{\AA}$	8.481(2)	8.750(1)	8.989(2)	8.765(1)
$b/\text{\AA}$	18.499(3)	9.898(1)	10.154(2)	10.284(1)
$c/\text{\AA}$	11.469(3)	11.342(1)	11.223(2)	11.180(1)
$\alpha/\text{deg}$	90	89.77(1)	64.30(1)	63.95(1)
$\beta/\text{deg}$	106.88(2)	72.74(1)	72.27(1)	73.48(1)
$\gamma/\text{deg}$	90	68.64(1)	88.90(1)	89.30(1)
$V/\text{\AA}^3$	1721.8(7)	867.6(2)	871.6(3)	860.5(2)
$Z$	2	1	1	1
$S$	1.699	1.511	1.259	1.159
$R_1$	0.0636	0.0521	0.0357	0.0595

by organic solids and shown how stereoselective reactions can be achieved by microporous organic molecular crystals.<sup>15</sup> Toda has been a proponent of solid–solid reactions with organic compounds and has carried out a large number of transformations, often with remarkable selectivity.<sup>16</sup>

(15) (a) Sawaki, T.; Endo, K.; Kobayashi, K.; Hayashida, O.; Aoyama, Y. *Bull. Chem. Soc. Jpn.* **1997**, *70*, 3075. (b) Endo, K.; Koike, T.; Sawaki, T.; Hayashida, O.; Masuda, H.; Aoyama, Y. *J. Am. Chem. Soc.* **1997**, *119*, 4117. (c) Dewa, T.; Endo, K.; Aoyama, Y. *J. Am. Chem. Soc.* **1998**, *120*, 8933. (d) Sawaki, T.; Aoyama, Y. *J. Am. Chem. Soc.* **1999**, *121*, 4793. (e) Sawaki, T.; Dewa, T.; Aoyama, Y. *J. Am. Chem. Soc.* **1998**, *120*, 8539.

We have carried out the solid–solid reaction between the host (H) and each of the aminobenzonitrile guests in turn, starting with H:G ratios of 1:2.

(16) (a) Toda, F. *Pure Appl. Chem.* **1996**, *2*, 285–290. (b) Im, J.; Kim, J.; Kim, S.; Hahn, B.; Toda, F. *Tetrahedron Lett.* **1997**, *38*, 451–452. (c) Toda, F.; Hyoda, S.; Okada, K.; Hirotsu, K. *J. Chem. Soc., Chem. Commun.* **1995**, 1531–1532. (d) Toda, F.; Miyamoto, H. *Chem. Lett.* **1995**, 809–810. (e) Toda, F.; Miyamoto, H. *Chem. Lett.* **1995**, 861. (f) Kaupp, G.; Haak, M. *J. Phys. Org. Chem.* **1995**, *8*, 545–551. (g) Toda, F.; Okuda, K.; Fujiwara, T. *Mol. Cryst. Liq. Cryst.* **1992**, *219*, 157–161. (h) Toda, F.; Takumi, H.; Yamaguchi, H. *Chem. Exp.* **1989**, *4*, 507–510. (i) Toda, F.; Mori, K. *J. Chem. Soc., Chem. Commun.* **1989**, 1245–1246.

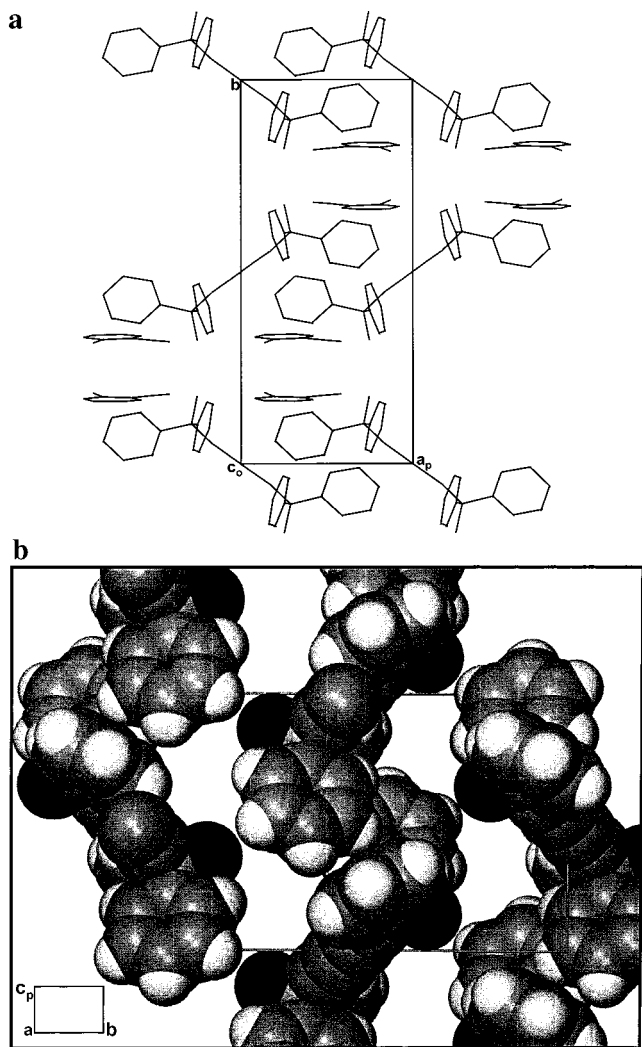


**Figure 2.** (a) Projection of **1** along [001]. (b) Space-filling projection of **1** along [100] with guest molecules omitted, showing the open channels.

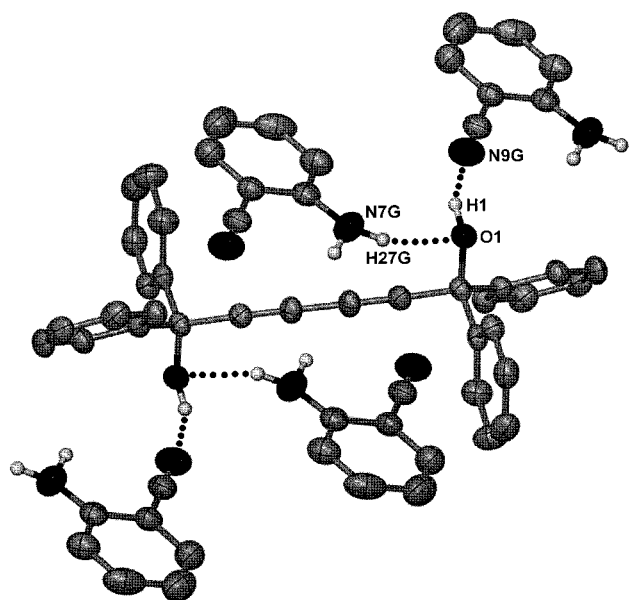


**Figure 3.** Hydrogen bonding scheme for **1**.

In each case grinding for 20 min at room temperature yielded a product that had the same structure as that found in the host–guest compound grown as single crystals from solution.

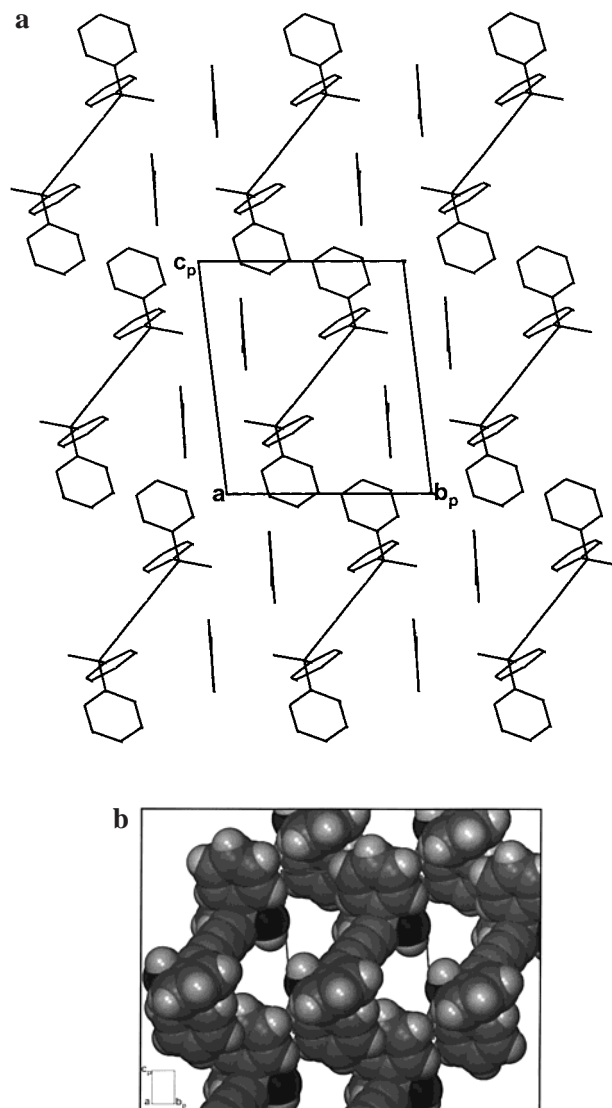


**Figure 4.** (a) Projection of **2** along [100]. (b) Space-filling projection of **2** along [100] with guest molecules omitted, showing the open channels.

This was checked by analysis of the measured X-ray powder diffraction pattern of the ground product, which we compared with the calculated pattern derived from the single-crystal structure (LAZYPULVERIX<sup>17</sup> program). A typical example is shown in Figure 9. The match is convincing in that all the strongest peaks are present at the correct angular position and the intensities are in general agreement.

Interestingly, it is possible to use solid–solid reactions to carry out competition experiments and displacement reactions. We have used this technique in the study of cocrystal formations between a sulfonamide and aromatic carboxylic acids.<sup>18</sup>

We ground the host compound with mixtures of two guests, G1 and G2 with variable mole fraction of G1. We separated the host–guest compounds and analyzed the G1:G2 ratio. The results are shown in Figure 1.

For the 2ABN/3ABN solid–solid competition reaction (Figure 1a) the 2ABN isomer is clearly favored. This is repeated in the 2ABN/4ABN case where 2ABN is again preferentially enclathrated. However, in the 3ABN/4ABN experiment, there

(17) Yvon, K.; Jeitschko, W.; Parthé, E. *J. Appl. Crystallogr.* **1977**, *10*, 73.

(18) Caira, M. R.; Nassimbeni, L. R.; Wildervanck, A. F. *J. Chem. Soc., Perkin 2* **1995**, 2213–2216.

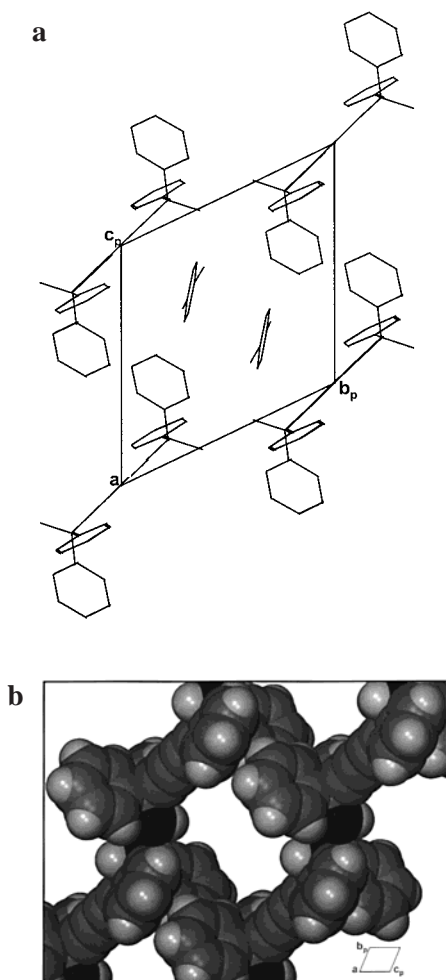


**Figure 5.** (a) Projection of **3** along [100]. (b) Space-filling projection of **3** along [100] with guest molecules omitted, showing the open channels.

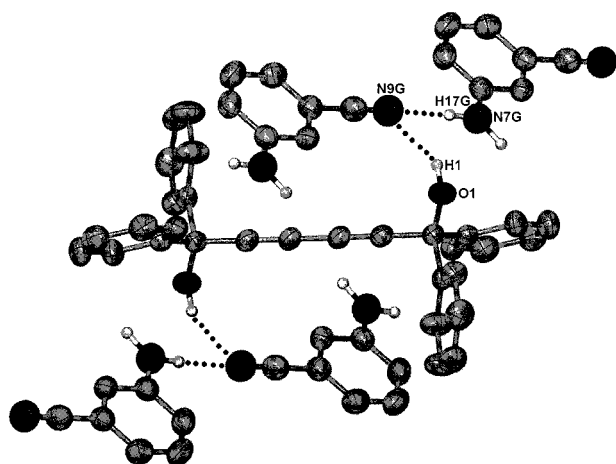


**Figure 6.** Hydrogen bonding scheme for **2**.

is virtually no preferential inclusion and the resulting points are close to the diagonal line representing zero selectivity.

Finally, we carried out a displacement reaction whereby we grew the inclusion compound  $\text{H}\cdot 2(3\text{ABN})$  from solution and ground the crystals with 2ABN.



This is the expected product, because it has the more negative

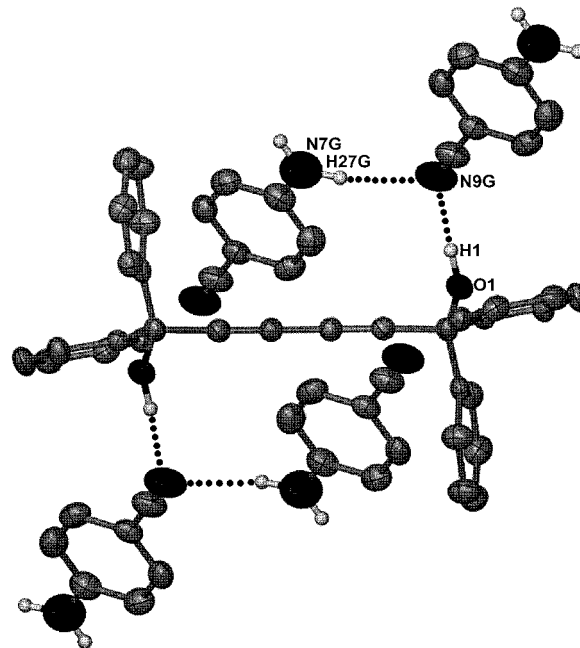


**Figure 7.** Hydrogen bonding scheme for **3**.

**Table 2.** Hydrogen-Bonding Parameters

compd	donor (D)	acceptor (A)	D–H/Å	D⋯A/Å	D⋯H–A/deg
<b>1</b>	O1	N9G	0.970(3)	2.891(3)	163(5)
	N7G <sup>a</sup>	O1	0.970(3)	3.193(5)	161(3)
<b>2</b>	O1	N9G	0.970(3)	3.312(3)	154(4)
	N7G <sup>a</sup>	N9G	0.970(3)	3.109(4)	177(2)
<b>3</b>	O1	N9G	0.970(3)	2.918(4)	178(3)
	N7G <sup>b</sup>	N9G	0.970(3)	3.258(5)	169(3)
<b>MIX</b>	O1	N8G	0.970(3)	2.897(4)	173(3)
	N10G <sup>a</sup>	N8G		3.136(5)	

<sup>a</sup>  $x - 1, y, z$ . <sup>b</sup>  $x + 1, y, z$ .

**Table 3.** Thermal Analysis and Lattice Energy Data

Inclusion compd	<b>1</b>	<b>2</b>	<b>3</b>
dissolution temp (°C)			
peak	123	101	81
onset	121	99	79
lattice energy (kJ mol <sup>-1</sup> )	-550.7	-504.1	-489.0
$\Delta H$ (J g <sup>-1</sup> )	150	104	71

lattice energy. We checked our hypothesis by attempting the reverse reaction, but the product was identical to the starting material



showing that displacement had not taken place.

The solid-state reactions are indeed gratifying in that they follow the trends obtained in the solution experiments and the DSC dissolution temperatures, all being dictated by the trends in the lattice energies.

## Experimental Section

The inclusion compounds **1**, **2**, and **3** were obtained by dissolving the host compound (**H**) and the solid guest in the minimum amount of 1-butanol. Suitable quality crystals appeared by slow evaporation over a period of 2 h to 10 days. Preliminary cell dimensions and space group symmetry were determined photographically and subsequently refined on a Nonius Kappa CCD diffractometer using graphite-monochromated Mo K $\alpha$  radiation. The strategy for the data collection was evaluated

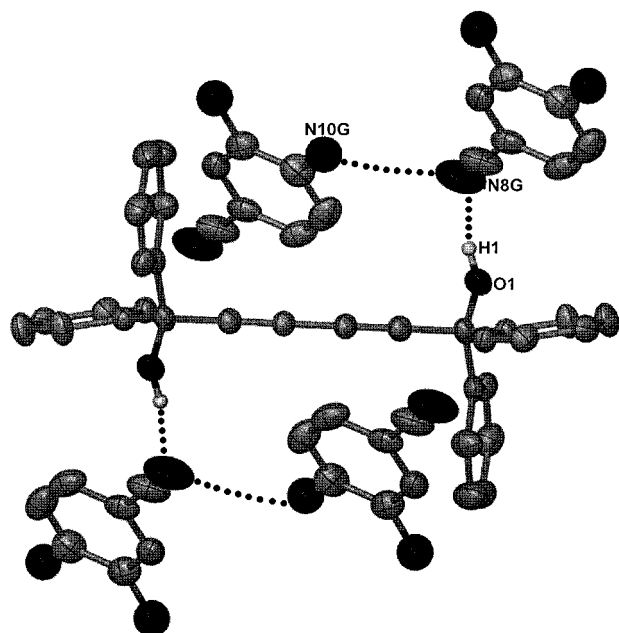


Figure 8. Hydrogen bonding scheme for MIX.

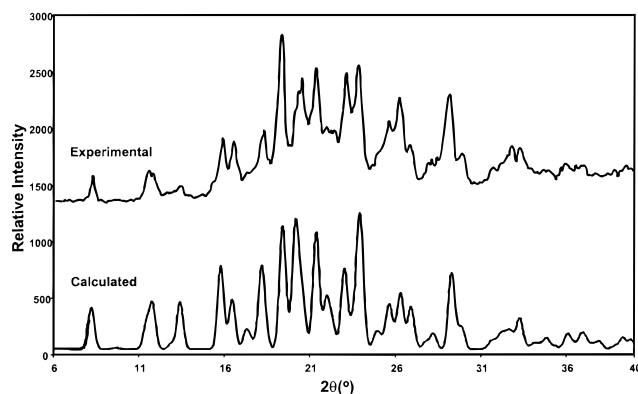


Figure 9. Experimental and calculated powder patterns for 2.

using the COLLECT<sup>19</sup> software. The detector to crystal distance for 1, 2, 3, and MIX was 40, 45, 40, and 47 mm, respectively. For all three structures data were collected by the standard  $\phi$  scan and  $\omega$  scan techniques. For each structure all sets of data were scaled and reduced using DENZO-SMN.<sup>20</sup> All three structures were solved by direct methods using SHELX-86<sup>21</sup> and refined employing full-matrix least-squares with the program SHELX-97<sup>22</sup> refining on  $F^2$ .

We also grew single crystals of the host with a mixture of 3ABN and 4ABN. We concentrated on obtaining relatively large single crystals (typically  $2 \times 2 \times 0.5 \text{ mm}^3$ ) so that we could cut such a single crystal into portions and carry out crystal structure analysis and gas chroma-

(19) COLLECT, data collection software, Nonius, 1998.

(20) Otwinowski, Z.; Minor, W Processing of X-ray Diffraction Data Collected in Oscillation Mode. *Methods in Enzymology*; Carter, C. W., Jr., Sweet, R. M., Eds.; Academic Press: New York, 1997; Vol. 276, Macromolecular Crystallography, Part A, pp 307–326.

(21) Sheldrick, G. M. SHELX-86. In *Crystallographic Computing 3*; Sheldrick, G. M., Kruger, C., Goddard, R., Eds.; Oxford University Press: Oxford, 1985; p 175.

tography from the same single crystal. This is an important point, because inclusion compounds in general, and the ones with mixed guests in particular, are notoriously nonstoichiometric. We have had the experience of growing batches of single crystals from mixed guests where the ratio of the included guests varies not only from batch to batch but also within the same batch of crystals.

**Competition Experiments.** Competition experiments were carried out between pairs of guests as follows:

For the competition by crystallization from solution, a series of 11 vials were made up with mixtures of two guests such that the mole fraction of a given guest varied from 0 to 1. Host compound was added to each mixture, keeping the ratio of host to total guest at 1:18, and allowed to dissolve in 1-butanol by warming. The vials were left open at room temperature. The resulting crystalline inclusion compounds were filtered, dried, and placed in vials with silicone seals. The crystals were heated to release the guest mixtures, which were then analyzed by gas chromatography.

The experiment was extended to analyze simultaneous competition by all three isomers. Initial mixtures of all three guests were selected on an inner triangle drawn on a triangular diagram representing the competitions of the isomers as shown in Figure 1d. The equi-mixture of the guests, with 1/3 mole fraction each, representing the center of the inner triangle, was also analyzed. The crystalline inclusion compounds obtained were analyzed as before.

For the solid-state competition experiments we prepared guest mixtures of two guests, G1 and G2, with selected values of the mole fraction of G1 varying between 0 and 1 and keeping the moles of total guest 20 times in excess of the moles of host. We achieved a phase separation of the resultant host–guest compound by addition of dilute HCl. The excess guest formed an oil, while the host–guest compound formed a fine white precipitate which was filtered, dried, and analyzed by gas chromatography as before. We carried out controlled experiments and showed that the pure host–guest complexes are stable toward HCl, and neither guest desorption nor decomposition occurs.

**Thermal Analysis.** Thermogravimetry (TG) and differential scanning calorimetry (DSC) were carried out on a Perkin-Elmer PC7-Series system. These experiments were performed over a temperature range of 30–300 °C at a heating rate of 10 °C min<sup>-1</sup> with a purge of dry nitrogen flowing at 30 mL min<sup>-1</sup>. The samples were crushed, blotted dry, and placed in open platinum pans for TG experiments and in crimped but vented aluminum pans for DSC.

**X-ray Powder Diffraction (XRD).** X-ray powder diffraction patterns were measured using the Philips PW3710 under mpd control. Nickel-filtered Cu K $\alpha$  radiation was used. A step size of 0.1° at a scan rate of 2 s per step in the  $2\theta$  range from 6 to 40° was employed.

**Acknowledgment.** We thank the National Research Foundation (Pretoria) and Sastech for Research Grants.

**Supporting Information Available:** Tables of fractional atomic coordinates and thermal parameters, anisotropic displacement parameters, bond lengths, bond angles, fractional coordinates for hydrogen atoms and isotropic thermal parameters, and torsion angles for 1–3 and MIX (PDF). This material is available free of charge via the Internet at <http://pubs.acs.org>.

JA994066+

(22) Sheldrick, G. M.; Schneider, T. R. SHELXL: High-Resolution Refinement. *Methods in Enzymology*; Carter, C. W., Sweet, R. M., Eds.; 1997; Vol. 277, Macromolecular Crystallography Part B, pp 319–343.